

AD A 126697

DTIC FILE COPY

Nonequilibrium water permeation in SiO₂ thin films

Robert Pfeffer, Robert Lux, and Harry Berkowitz
U. S. Army Electronics Technology and Devices Laboratory (ERADCOM), Fort Monmouth, New Jersey 07703

W. A. Lanford and C. Burman
Department of Physics, State University of New York, Albany, New York 12222

(Received 6 January 1982; accepted for publication 21 February 1982)

Nuclear resonance profiling was used to measure the distributions of hydrogen incorporated into dry SiO₂ films by thermal treatments in steam. Thermal oxides were grown on silicon to a thickness of 260 nm in dry O₂ and were subsequently treated in steam at temperatures of 320 and 500°C for periods lasting between 390 and 6 × 10⁵ s. The concentrations of hydrogen carried in by permeating water were then profiled with 6.4 MeV ¹⁵N ions using the resonant nuclear reaction ¹H(¹⁵N, αγ)¹²C. Water was seen to penetrate the films rapidly and to slowly react with the SiO₂ uniformly throughout the films. Two distinct stages were observed in the buildup of H, indicating that the water/SiO₂ reaction involves at least two concurrent processes rather than a single-stage process.

PACS numbers: 66.30. - h, 68.60. + q, 81.60.Dq

Thermal oxidation of silicon to form high-quality insulating films of SiO₂ is an important process in modern electronic technology. The properties of the oxides formed by this process have been found to depend critically on the presence of water absorbed in the films either during oxidation or in subsequent high temperature processing. An example of this is the recent observation¹ of morphological differences between wet and dry ultra-thin metal-oxide-semiconductor (MOS) gate oxides: wet films were seen to be free of the micropores present in dry films and showed better breakdown resistance. Physical models of the diffusion and incorporation of water in SiO₂ have received comparatively little experimental testing. In an early study of water diffusion in fused silica, Moulson and Roberts² proposed that the transport involved mobile OH groups arising from the reaction



at the outer surface. They modeled the process with Fick's second equation using a constant effective diffusion coefficient

$$\partial [\text{OH}]/\partial t = D_{\text{eff}} \nabla^2 [\text{OH}], \quad (2)$$

determining D_{eff} by observing the time behavior of the total OH content during the early stages of steam absorption and vacuum desorption. An alternative model, proposed by Doremus,³ was the transport of dissolved molecular water through "doorways" between cells or interstices in the network, with the SiOH groups produced by reaction (1) being *immobile*. He also assumed (a) that the reaction proceeded rapidly compared to diffusion, allowing the equilibrium concentrations of diffusing water and SiOH groups to be related by the law of detailed balance

$$[\text{H}_2\text{O}] = [\text{OH}]^2 / K^2, \quad (3)$$

and (b) that the water concentration and its time derivative were negligible compared to those for SiOH. These assumptions led him to model the process with the concentration-dependent diffusion equation

$$\partial [\text{OH}]/\partial t = (2D/K^2) \nabla^2 [\text{OH}]^2, \quad (4)$$

where D and D_{eff} are related by $D_{\text{eff}} = 2D [\text{H}_2\text{O}]/[\text{OH}]$. This produced a much better match to the [OH] profiles measured by Roberts and Roberts⁴ in fused silica than is possible with a solution to Eq. (2). (A profile measured by Moulson and Roberts was insufficiently precise to distinguish the two models.) This model, unlike the earlier one, also implies a larger effective diffusivity for absorption than for desorption, consistent with the measurements of Moulson and Roberts. Doremus also used this model to treat the steady-state steam oxidation of silicon,⁵ relating the temperature and pressure dependence of the parabolic oxidation-rate constant to that of D_{eff} .

Doremus' model applies to the regime where equilibrium has been established between [H₂O] and [OH]. Our previous observations⁶ of tracer ¹⁸O exchange during water diffusion at relatively low temperatures were generally consistent with this model. However, we saw evidence of a systematic trend toward anomalously low exchange rates during the early stages of absorption in dry oxides. This suggested that the [OH] had not reached its saturation value, contrary to our expectation from Eq. (4) that it should have reached it on a time scale of x_0^2/D_{eff} , where x_0 is the film thickness. We therefore decided to investigate the early behavior of water absorption in dry oxides.

Samples were prepared by forming thermal oxide films in nominally dry O₂ at 1100 C on (100) surfaces of 5 Ω cm (nominal) *n*-type silicon to a thickness of 260 nm. The samples were subsequently treated in flowing steam at 1 atm according to the procedure described in Ref. 6. Formation of additional oxide during the steam treatments was negligible. The concentrations of hydrogen carried in by absorbed water were then profiled with 6.4 MeV ¹⁵N⁺ ions⁷ by detecting the characteristic 4.4-MeV gamma rays from the resonant nuclear reaction ¹H(¹⁵N, αγ)¹²C. The beam current was about 40 nA and the beam spot was about 3 × 10 mm, producing negligible sample heating. Data collection lasted about 8 min at each beam energy. The integrated ion-beam current was 24 μC at each beam energy.

Detailed profiles of the near-surface regions showed

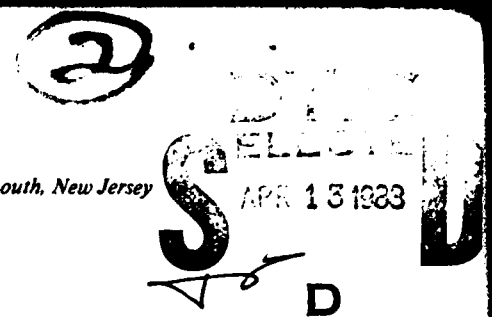


TABLE I. Observed yield of 4.43 gamma rays emitted from reactions occurring at indicated depths in 260-nm SiO₂ films: number of counts recorded per 24 μ C of incident ¹⁵N ions.

Sample	Treatment temp. (C)	Time (s)	Counts at depths in films (nm)					
			80	140	199	229	258	288
201	500	96 030	329	280	283	256	242	78
202	500	29 160	256	211	221	219	208	43
203	500	14 160	250	201	206		211	45
204	500	4 350	241	172	202		159	32
205	500	1 860	209	193	139		114	43
301	320	601 320	382	329	328	306	243	51
302	320	167 700	286	268	240	221	162	41
303	320	57 600	217	235	212	164	147	43
304	320	21 600	249	216	179	165	90	30
305	320	7 320	210	198	175		132	48
306	320	2 760	218	193	151		94	46
307	320	1 020	145	131	94		82	48
308	320	390	121	114	86		69	34
309	Untreated		131		72*		30	

*At depth of 170 nm.

that a hydrogenous layer about 5 nm thick coated the surface of every sample, including an unoxidized Si sample which was profiled to determine instrumental background. This layer, which commonly forms on SiO₂ surfaces exposed to air, allowed us to determine the effects of beam spread, energy straggling, and resonance width on the depth resolution of the profile. A yield curve of gamma rays collected from the layer was matched to a theoretically obtained curve generated by assuming a Lorentzian resonance in the cross section. The best fit to its effective width was about 8 keV, corresponding to a depth resolution of about 5 nm near the surface; energy straggling approximately doubled this near the oxide-silicon interface. The [H] was therefore sampled only every 30 nm and no closer than 80 nm to the surface to avoid contributions from the hydrogenous outer layer.

Some difficulties have been reported by other investigators involving changes in H profiles induced by nuclear profiling; these have included hydrogen effusion⁸ from *a*-Si and room-temperature vacuum desorption of water from some soda-lime glasses.⁹ To check for these effects, data collection from points sampled early was repeated after completion of profiling. No statistically significant variations in [H] were observed, either in the interior or at the surface.

Our profiling results are listed in Table I, which shows the number of counts recorded from reactions occurring at various depths below the base of the hydrogenous layer (depths were calculated using a specific energy loss of 1.69 MeV/ μ m). The samples are in two groups, one whose treatments were at 500 C and the other at 320 C; also shown is an oxidized but untreated sample (number 309). An unoxidized silicon sample (not shown) was included for background determination; this yielded about 36 counts at every depth. After background subtraction, the counts were converted to H concentrations with calibration data obtained from previous measurements of samples containing known quantities of hydrogen.¹⁰ Some representative profiles are plotted in Fig. 1; the error bars indicate statistical uncertainty.

These results show that the [H] profiles are essentially uniform throughout the oxides, rather than taking the form

of advancing fronts of diffusant. This is clearly contrary to the prediction of the Fickian OH-diffusion model, Eq. (2). In the context of the molecular H₂O diffusion/reaction model, it indicates that chemical equilibrium had *not* been achieved during the permeation process, invalidating Eq. (4) as well. This can be seen by inspection of Fig. 2, in which are plotted the profiles predicted by solving those equations. The relative flatness of the observed profiles is an indication that the diffusion through the oxides was rapid compared to the reaction, allowing the diffusant concentration to approach uniformity before any appreciable quantity of product had built up. The one exception observed was the oxidized but untreated sample, which shows a small but detectable accumulation of H near the surface; this may have entered the oxide immediately after its formation.

The relative uniformity of the distributions under the conditions of this experiment (i.e., thin films and moderate

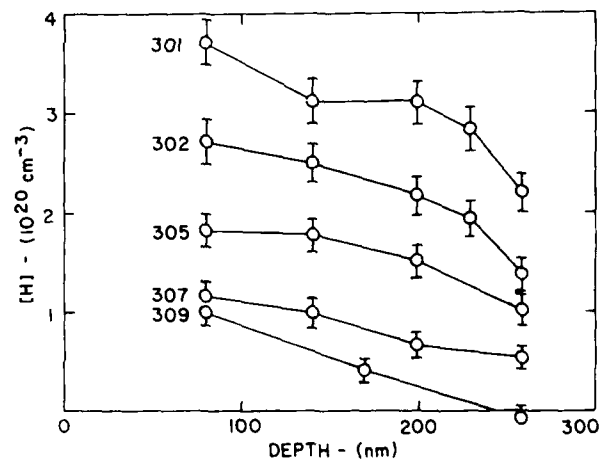


FIG. 1. Representative [H] profiles measured with 6.4-MeV ¹⁵N ions for some samples listed in Table I. All samples were 260-nm thick oxides which had been thermally grown in nominally dry O₂ at 1200 C and then treated in 320 C steam at 1 atm for the durations indicated.

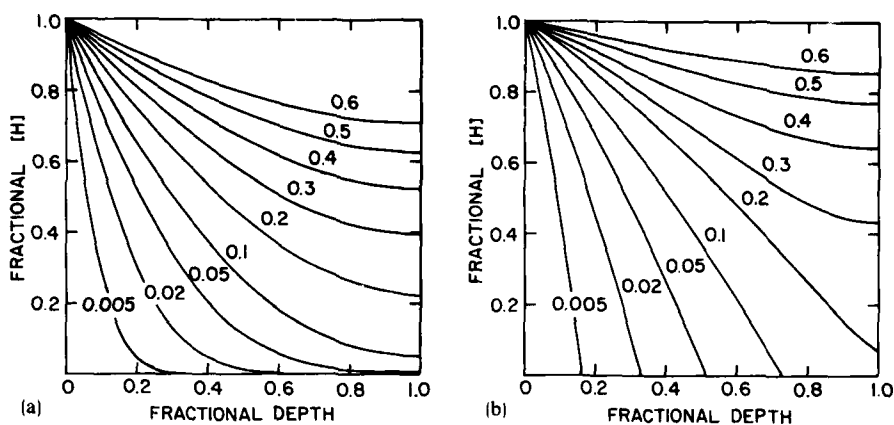


FIG. 2. Theoretical [H] profiles at various times for diffusion into an initially dry oxide film of thickness x_0 , normalized to [H] at infinite time. Curve labels denote time, which is expressed in units of x_0^2/D . The profiles shown in (a) were obtained by solving Eq. (2), and those in (b) were obtained by solving Eq. (4) with $K = 2$; the boundary conditions were in both cases $[H] (\text{surface}) = 1$ and $\partial[H]/\partial x (\text{interface}) = 0$. They may be compared to the corresponding profiles given by Crank for an infinite medium (see Ref. 11).

temperatures) enabled the hydration process to be singled out for study independently of diffusion. For this purpose, the measured data was summarized by averaging for each steam treatment the [H] in the interiors of the oxide films. Results of this procedure appear in Fig. 3, which may be regarded in this context as an example of a Powell-plot¹² used for reaction-rate law determination. Note that a break clearly occurs in the curve of [H] vs t for either treatment temperature, implying that the hydration of SiO_2 involves at least a dual rather than a single reaction. One component reaction appears to approach completion before the other has contributed significantly: the value of [H] arising from the fast component appears to saturate at about $1.5 \times 10^{20} \text{ cm}^{-3}$ at 320 C. This is well below our projection of $4.1 \times 10^{20} \text{ cm}^{-3}$ for the equilibrium concentration at that temperature, which we obtained by extrapolating the plot of OH solubility versus temperature calculated by Shackelford and Masaryk.¹³ (We are aware that other investigators have obtained different results.) At 500 C the fast component appears to saturate at $2 \times 10^{20} \text{ cm}^{-3}$, accounting for most of the projected equilibrium concentration of $2.5 \times 10^{20} \text{ cm}^{-3}$. A rough estimate of the activation energies can be obtained from the buildup rates for the products of the component

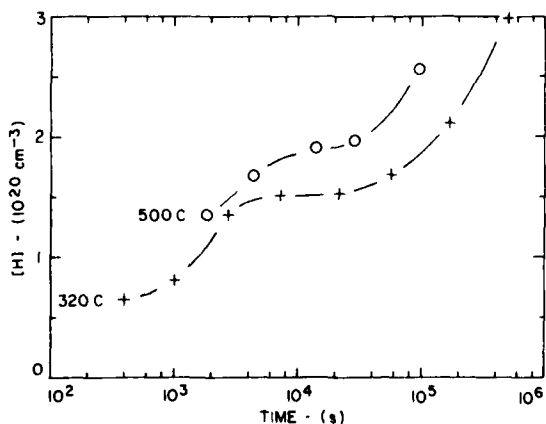


FIG. 3. Mean [H] observed in steam-treated oxide films as functions of treatment duration at fixed temperatures indicated. (The curves connecting the points are intended only as viewing guides.)

reactions at different temperatures. This procedure yielded respective activation energies of approximately 0–2 and 15–18 kcal/mol for the fast and slow components, respectively.

Although the details of the hydration process are not yet fully clear, the results of this and related experiments allow some inferences to be drawn. Our evidence for a multi-component reaction is consistent with the results of Walrafen and Samanta,¹⁴ who showed that the 3690-cm^{-1} OH stretching contour which they observed in the Raman and infrared absorption spectra of fused silica could be decomposed into as many as four distinct components. The low activation energy which we infer for our fast component is consistent with their suggestion that hydrogen bonding plays an important role in the reaction; its magnitude is typical of those associated with that type of bonding.¹⁵ The comparative rapidity of that component reaction and its limited extent suggest the possibility that it represents hydrogen bonding between network oxygen and molecular water. The higher activation energy of the slow component suggests its interpretation as the dissociation reaction which Mikkelsen¹⁶ recently observed to produce complete oxygen exchange between network SiO_2 and diffusing water, excluding the possibility of a limited number of fixed saturable sites for that reaction. Further clarification of the hydration mechanism awaits more detailed studies of reaction-product evolution. These are now in progress, as are model calculations of total H buildup and ^{18}O exchange kinetics.

ACKNOWLEDGMENTS

We would like to express our appreciation to R. H. Doremus for his encouragement and assistance, and J. C. Mikkelsen, Jr. for useful discussions.

¹J. M. Gibson and D. W. Dong, *J. Electrochem. Soc.* **127**, 2722 (1980).

²J. Moulson and J. P. Roberts, *Trans. Faraday Soc.* **57**, 1208 (1961).

³R. H. Doremus, *Glass Science* (Wiley, New York, 1973), p. 134ff.

⁴G. J. Roberts and J. P. Roberts, *Phys. Chem. Glasses* **5**, 26 (1964); **7**, 82 (1966).

⁵R. H. Doremus, *J. Phys. Chem.* **80**, 1773 (1976).

⁶R. Pfeffer and M. Ohring, *J. Appl. Phys.* **52**, 777 (1981).

⁷W. A. Lanford, H. P. Trautvetter, J. F. Ziegler, and J. Keller, *Appl. Phys. Lett.* **28**, 566 (1976).
⁸M. Fallavier, J. P. Thomas, J. Tousset, Y. Monteil, and J. Bouix, *Appl. Phys. Lett.* **39**, 490 (1981).
⁹R. H. Doremus, W. A. Lanford, and C. Burman (unpublished).
¹⁰W. A. Lanford, *Solar Cells* **2**, 351 (1980).
¹¹J. Crank, *The Mathematics of Diffusion*, 2nd ed. (Clarendon, Oxford, 1975), pp. 119-125.

¹²I. R. Levine, *Physical Chemistry* (McGraw-Hill, New York, 1978), p. 489.
¹³J. F. Shackelford and J. S. Masaryk, *J. Noncryst. Sol.* **21**, 55 (1976).
¹⁴G. E. Walrafen and S. R. Samanta, *J. Chem. Phys.* **69**, 493 (1978).
¹⁵S. N. Vinogradov and R. H. Linnell, *Hydrogen Bonding* (Van Nostrand Reinhold, New York, 1971); also Ref. 12, pp. 730, 785.
¹⁶J. C. Mikkelsen, Jr., *Appl. Phys. Lett.* **39**, 903 (1981).

Accession For	
NTIS GRA&I	<input checked="" type="checkbox"/>
DTIC TAB	<input type="checkbox"/>
Unannounced	<input type="checkbox"/>
Justification	
By	
Distribution/	
Availability Codes	
Dist	Avail and/or Special
A	21

